Multi-Resonance Mesh-Based Wavelength-Routed Optical Networks-on-Chip

Zhidan Zheng[◊], Liaoyuan Cheng[◊], Kanta Arisawa[*], Qingyu Li[◊], Alexandre Truppel[◊], Shigeru Yamashita[*], Tsun-Ming Tseng[◊], Ulf Schlichtmann[◊]
{zhidan.zheng,liaoyuan.cheng,qingyu.muc.li,alex.truppel,tsun-ming.tseng,ulf.schlichtmann}@tum.de, lucky@ngc.is.ritsumei.ac.jp,ger@cs.ritsumei.ac.jp
[◊]Technical University of Munich, Munich, Germany, [*]Ritsumeikan University, Kusatsu, Japan

ABSTRACT

Wavelength-routed optical networks-on-chip (WRONoCs) are well-known for providing high-speed and collision-free communication in multi-core processors. Previous work was unable to simultaneously reduce the design complexity and total optical power consumption of WRONoC. Besides, in current designs, each microring resonator (MRR), which is the key component of WRONoC, is configured to demultiplex to one specific wavelength. This significantly increases the MRR usage and the insertion loss. In this work, we adapt different types of ONoC routers into the mesh-based template. To reduce MRR usage, we take advantage of an important feature of MRR, multi-resonance, so that a single MRR can demultiplex signals on multiple wavelengths. To this end, we propose an efficient design method that synthesizes mesh-based WRONoCs using multi-resonance MRRs and existing optical routers to reduce total power consumption. The experimental results show that our method outperforms state-of-the-art design methods in significantly reducing MRR usage and optical power.

KEYWORDS

Wavelength-routed optical networks-on-chip, mesh structure, multi-resonance microring resonators.

1 INTRODUCTION

As the trend toward multi-core processors keeps growing, the power consumption issue is becoming increasingly important for communication in networks-on-chip (NoC). This challenge motivates the development of advanced interconnect technologies [1, 2]. Among them, optical NoCs (ONoCs) with silicon photonics raise great interest in both academia and industry [2]. Compared to conventional NoCs using metallic interconnects, ONoCs can provide higher bandwidth with lower power consumption [3].

In ONoCs, signal transmission relies on two key components: *waveguides*, where optical signals are transmitted, and *microring resonators* (MRRs) that can demultiplex signals from waveguides [4].

DAC '24, June 23–27, 2024, San Francisco, CA, USA

ACM ISBN 979-8-4007-0601-1/24/06…$15.00
https://doi.org/10.1145/3649329.3655914

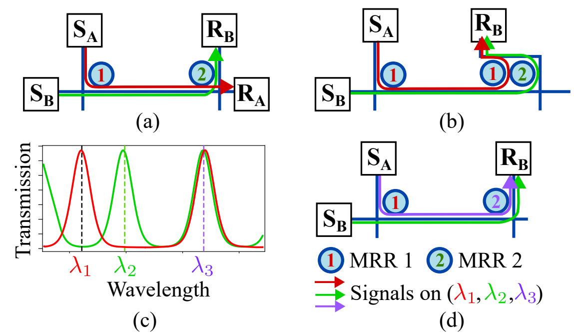

Figure 1: (a) Signal on λ_1 from sender S_A to receiver R_A and signal on λ_2 from sender S_B to receiver R_B. (b) S_A and S_B communicate to R_B using signals on λ_1 and λ_2, respectively. (c) MRR 1 resonates to $\{\lambda_1, \lambda_3\}$, and MRR 2 resonates to $\{\lambda_2, \lambda_3\}$. (d) S_A communicates to R_B using the signal on λ_3.

Specifically, optical signals on multiple wavelengths can be transmitted along a waveguide simultaneously thanks to the wavelength-division multiplexing technology [5]. If a signal approaches an MRR and the wavelength of the signal matches the resonant wavelengths of the MRR, the signal is coupled to the MRR and turned to another waveguide; otherwise, the signal keeps its original transmission direction. Among ONoCs, wavelength-routed ONoCs (WRONoCs) are well-known for providing collision- and reconfiguration-free communications. In WRONoCs, the signal paths from senders to receivers are well-designed and fixed during the design phase [5, 6]. Therefore, all signals can be transmitted at the same time without data collision [3, 7, 8]. Figure 1(a) shows a simple WRONoC network that supports simultaneous communications from sender S_A to receiver R_A and from sender S_B to receiver R_B. In particular, the signals from both senders use two different wavelengths, λ_1 and λ_2, and two MRRs are configured to resonate to λ_1 and λ_2, respectively.

There are several design automation approaches for WRONoCs. As the first method that simultaneously considers both topological and physical aspects of WRONoCs, the PSION family of tools [8–10] refine the design space based on customized templates and improve energy efficiency by reducing MRR usage. However, with these tools, computational complexity increases exponentially with network size. For instance, PSION+ can synthesize an 8-core network in a few seconds, whereas synthesizing a 16-core network requires six days. For the networks integrating more cores that meet today's communications requirements, these tools can hardly obtain the optimal solutions within reasonable time. CoDesign[7] presents a WRONoC design method that significantly reduces computational complexity and synthesis time. However, this method requires high

MRR usage. For example, in a 16-core network, PSION+ requires 320 MRRs, while CoDesign requires 544 MRRs. This high usage of MRRs introduces considerable tuning power to support their operation, which increases the overall power consumption. Thus, no method has been able to simultaneously reduce WRONoC computational complexity and total optical power consumption while minimizing the use of MRRs.

Given the above challenges, we adopt an easily extensible mesh structure as a design template. On the template, the locations of optical routers and their interconnection are fixed, which greatly reduces computational complexity. To enable multidirectional signal routing among cores on the template, we equip each core with a router. These routers are not limited to WRONoC types and have proven efficient communication. Building on this, we integrate, for the first time, different types of ONoC routers into the mesh-based template, which enables flexible signal routing with lower power consumption and computational complexity in WRONoC design.

To reduce MRR usage, we take advantage of the *multi-resonance MRR* for signal routing. As described in [11, 12], an important feature of MRRs is that a single MRR can resonate to multiple wavelengths. However, in current WRONoC designs, each MRR is configured to resonate to only one specific wavelength. This configuration results in massive MRR usage. As shown in Figure 1(b), if the signals from two senders S_A and S_B need to be coupled at the same place and reach receiver R_B, two different MRRs are required, which increases tuning power for MRRs and insertion loss. With the help of multi-resonance MRRs, we can reduce MRR usage. For example, Figure 1(c) shows the transmission spectra of two MRRs: MRR 1 resonates to λ_1 and λ_3, while MRR 2 resonates to λ_2 and λ_3. That is, both MRRs can resonate to λ_3. To avoid data collisions, as shown in Figure 1(d), we set the signals from senders S_A and S_B on λ_3 and λ_2, respectively. This allows the signals to reach R_B without extra MRRs, effectively reducing the MRR usage compared to the scenario in Figure 1(b).

In this work, we propose an efficient design method that synthesizes mesh-based WRONoCs using multi-resonance MRRs and existing optical routers to reduce total power consumption. Our method consists of two steps. First, we construct a mesh-based network and route signals for the required communications. Specifically, we apply *XY/YX routing* algorithm to route signals with minimized path lengths and adapt existing optical routers to support signal routing with the optimized MRR usage. Second, we apply multi-resonance MRRs for the signals that need to be coupled at the same places without introducing extra MRRs. Moreover, we assign the wavelengths to the signals and configure the radii of MRRs carefully without causing data collisions. We compared our method to two state-of-the-art design methods: PSION+ [8] and CoDesign [7] for a real WRONoC benchmark. The experimental results show that, similar to CoDesign, our method can synthesize a 16-node network in a few seconds. In addition, our method reduces the MRR usage by 68% and 81% compared to PSION+ and CoDesign, respectively. With the minimized MRR usage, our method outperforms PSION+ and CoDesign, reducing the total optical power by about 13%.

2 FRAMEWORK

In this section, we introduce all necessary elements of our work.

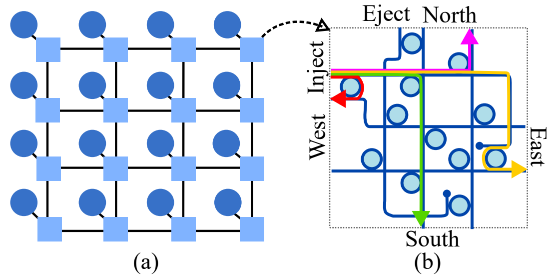

Figure 2: (a) A mesh-based network with 16 cores. (b) A 5×5 optical router, where four signals, represented by red, green, yellow, and pink lines, are injected to other four directions: west, south, east, and north, respectively.

2.1 Mesh Structure

In this work, we adopt the mesh structure as a design template. In a mesh-based network, cores are regularly aligned and managed into a grid form [13, 14]. Each core has a dedicated router to communicate with other cores. Figure 2(a) shows a 16-core mesh-based network. Considering that the way of connecting routers is deterministic, when the number of cores increases, the mesh structure can easily be extended by adding more rows or columns of cores and routers without complex redesign. Besides, in the mesh structure, the connections among routers and the positions of routers are fixed, which greatly reduces computational complexity.

2.2 Optical Routers

We consider efficient ONoC routers that are customized for mesh structure and support signal transmission in five directions. Figure 2(b) shows a representative active ONoC router called OXY [15], which has five ports to support signals from five directions: injection/ejection, north, east, south, and west. Among the five ports, OXY provides *full connectivity*, i.e. one input can send signals to any other outputs. This makes it applicable to various communication needs. In addition, OXY optimizes MRR usage and energy efficiency. Besides OXY, we use two other 5-port active ONoC routers, Crux [14] and Cygnus [16], and two 4-port WRONoC routers, GWOR [17] and Light [6], and propose a 3-port router by ourselves.

2.3 Multi-Resonance MRRs

As introduced earlier, an MRR has multi-resonance feature. In particular, an MRR is formed by a looped waveguide, and its resonance condition is determined by the radius of the MRR and the wavelength of the signal [5, 11, 18]. When the round trip length of the MRR is an integer multiple of the wavelength of a signal, resonance occurs. Within a certain wavelength band, the circumference of an MRR can be an integer multiple of different wavelengths, resulting in multiple resonant wavelengths for the MRR without introducing extra energy or area cost [12]. Similarly, for a specific wavelength and a range of MRR radii, MRRs of different round trip lengths can be integer multiples of it and resonate to it, indicating that a single wavelength can be the resonant wavelength of multiple MRRs.

In this work, we use the same wavelength band, the range of MRR radii, and the resonant wavelengths of each MRR radius as applied in [11].

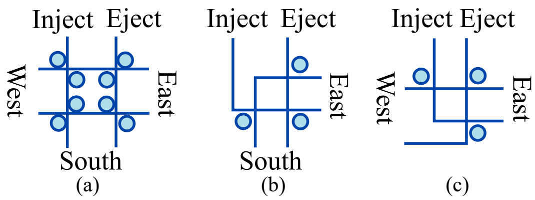

Figure 3: (a) A GWOR router has four ports. (b) Our proposed 3-port router. (c) The 3-port router supports signals from injection/ejection, east, and west.

2.4 Performance Factors

In ONoCs, optical power is positively related to MRR usage [1]. First of all, more MRRs indicate more tuning power. Typically, MRR thermal tuning power contributes 20%–60% to the total optical power, depending on the number of MRRs in the network [7, 19]. Besides, MRRs are important sources of insertion loss that determine the laser power in ONoCs [20]. Among the five typical loss types, *drop loss* and *through loss* are generated when signals are on- and off-resonance to MRRs, respectively. The other loss types are *propagation loss*, which depends on the length of waveguides that signals travel, *bending loss*, which depends on the number of passed waveguide bends, and *crossing loss*, which depends on the number of passed waveguide crossings. To improve energy efficiency, our work focuses on minimizing MRR usage and insertion loss.

3 METHODOLOGY

In this work, we propose a design method for WRONoCs based on the mesh structure, where each core is connected to an optical router. For the optical routers in our mesh-based networks, we adapt existing optical routers and create a *router-library* for those routers. Our method consists of two main steps:

- First, given the communication requirements among cores, we apply *XY/YX* routing algorithms to find all possible signal path options. We propose a mixed-integer linear programming (MILP) model to select the proper signal paths out of all path options and determine the optical routers that can support the selected signal paths. To improve energy efficiency, our MILP model has two optimization objectives: MRR usage and the worst-case insertion loss.
- Second, based on all selected signal paths and optical routers, we ensure collision-free communications by assigning wavelengths to the signal paths and configuring the radii of the MRRs. If multiple signals need to be on-resonance to an MRR, we make use of multi-resonance MRRs instead of increasing MRR usage. We propose an integer linear programming (ILP) model for the wavelength assignment and radius configuration. Our ILP model focuses on minimizing the number of wavelengths.

3.1 Signal Routing and Router Selection

3.1.1 Definition of our Router-Library. As introduced in Section 2.2, our router-library has three 5-port routers, two 4-port routers and a 3-port router. Figure 2(b), 3(a) and (b) show the representative 5-, 4-, and 3-port router, respectively. Besides the 5-port routers, the other routers can only support signals from certain directions. For example, the 4-port router shown in Figure 3(a) can only support signals from injection/ejection, east, south, and west. We denote a set of certain ports as a *port combination.* For 4- and 3-port routers, we rotate them to have various port combinations[1]. For example, we rotate the 3-port router shown in Figure 3(b) counter-clockwise by 90° so that the router can have another port combination, i.e. injection/ejection, east, and west, as shown in Figure 3(c).

3.1.2 Our MILP Model. For N cores, we index the cores in the network as $c_1, c_2, \ldots, c_N$ and store them in a set C. Considering that each core is connected to a router, we create a set R for N router and denote the router connected to c_i as r_i. For a $r_i \in R$, we denote the inputs and outputs as $I^d_{r_i}$ and $O^d_{r_i}$, where d denotes the five ports, i.e. $d \in \{inject/eject, north, south, east, west\}$. In our router-library, we consider a router with a certain port combination as a router option, denote it as t, and store it in a set R_{lib}.

We introduce the constraints in our MILP model to route signals and select routers as follows:

• *Signal Routing*

First of all, if a core c_i communicates to another core c_j, we apply the *XY/YX routing* algorithm to find possible signal path options in the mesh-based network. Specifically, for each communication, we consider at most two possible path options: either we first route it in the vertical direction, and then in the horizontal direction, or the other way around. Figure 4(a) shows a signal path option for the communication between c_i and c_j. There are two reasons to use the XY/YX routing algorithm: (1) the length of the signal paths routed by the algorithm is minimized, which optimizes the propagation loss; and (2) each communication has at most two signal path options, which reduces computational complexity and speeds up the synthesis process.

For a signal path option between c_i and c_j, we denote it as s and store it in a set S_{c_i,c_j}. To represent a signal path $s \in S_{c_i,c_j}$, we record its sequentially passed routers in a set R_s and the corresponding ports in another set P_s. The passed routers and ports of the signal path shown in Figure 3(a) are $R_s = \{r_i, r_k, r_j\}$ and $P_s = \{I^{inject}_{r_i}, O^{east}_{r_i}, I^{west}_{r_k}, O^{south}_{r_k}, I^{north}_{r_j}, O^{eject}_{r_j}\}$.

For each communication, we need to select exactly one signal path option. To model that, we introduce a binary variable b_s to indicate if a signal path s is selected or not and the following constraints:

$$\forall\ c_i,\ c_j \in C: \sum_{s \in S_{c_i,c_j}} b_s = 1 \tag{1}$$

For every communication, We store its signal path options in a set S for later use.

• *Router Selection*

In our mesh-based network, each router $r \in R$ needs to be implemented as a certain router option $t \in R_{lib}$. For example, Figure 4(b) - (d) shows three possible router options to implement the router r_i shown in Figure 4(a). To indicate if a router $r \in R$ is implemented as a router option $t \in R_{lib}$, we introduce a binary variable $b_{r,t}$ and introduce the following constraints to ensure that each router is implemented as exactly one router option:

$$\forall\ r \in R: \sum_{t \in R_{lib}} b_{r,t} = 1 \tag{2}$$

[1]A 4-port router has four port combinations: $\{x, n, e, w\}$, $\{x, e, w, s\}$, $\{x, n, e, s\}$, $\{x, n, s, w\}$, where x, n, e, s, and w denote injection/ejection, north, east, south, and west, respectively. A 3-port router has six port combinations: $\{x, n, e\}$, $\{x, e, w\}$, $\{x, n, w\}$, $\{x, n, s\}$, $\{x, e, s\}$, $\{x, s, w\}$.

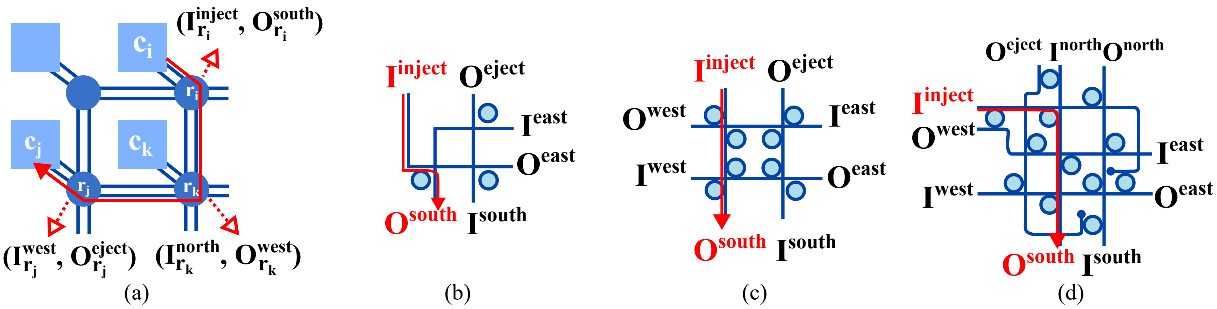

Figure 4: (a) A signal path option from c_i to c_j, which sequentially passes three routers, r_i, r_k, and r_j. (b) The signal path from I^{inject} to O^{south} suffers a bending loss and a drop loss in a 3-port router. (c) The signal path from I^{inject} to O^{south} suffers two crossing loss and four through loss in a 4-port router. (d) The signal path from I^{inject} to O^{south} suffers a drop loss, two through loss, and four crossing loss in a 5-port router.

For each $r \in R$, we need to ensure that the selected router option can support the signal paths passing through r. If a signal path passes a router from the direction that some router options do not support, those router options are invalid for the router. For example, for r_i, the 3-port router option shown in Figure 4(b) does not support the signals from north and west. The router option can be considered as a valid option for r_i only when no signals pass the north or west port. Thus, for each $t \in R_{lib}$, we create a set P_t for the ports that the router option **does not** have. For each $r \in R$, we check the signal paths that pass the d port, where $d \in \{inject/eject, north, south, east, west\}$ and store them in a set S^d_r. Then, we introduce the following constraints to prevent the invalid router options from being selected:

$$\forall\, r \in R,\ \forall t \in R_{lib},\ \forall d \in P_t,\ \forall\, s \in S^d_r:\ \ b_{r,t} + b_s \le 1 \tag{3}$$

• *MRR Calculation*

For a $r \in R$, an MRR in a $t \in R_{lib}$ is used only when the router option t is selected for this router r and at least a signal is on-resonance to the MRR. For each $r \in R$ and each $t \in R_{lib}$, we introduce a set $M_{r,t}$ for the MRRs if r is implemented as t. For each $m \in M_{r,t}$, we create a set S^{on}_m for the signals that are on-resonance to the MRR and use a binary variable b_m to indicate if m is used or not. We then introduce the following constraints:

$$\forall\, r \in R,\ \forall\, t \in R_{lib},\ \forall m \in M_{r,t},\ \forall s \in S^{on}_m:\ \ b_m \ge b_s + b_{r,t} - 1 \tag{4}$$

For the total number of MRRs, we use a integer variable i_{mrr} and model it as follows:

$$\forall\, r \in R,\ \forall\, t \in R_{lib}:\ \ i_{mrr} \ge \sum_{m \in M_{r,t}} b_m \tag{5}$$

• *Loss Calculation*

For the insertion loss of a signal path, we consider the five losses introduced in Section 2.4. We divide the calculation of the insertion loss into two steps. First, for a signal path, we calculate the length by summing the *Euclidean distance* between every two sequentially passed ports along the signal path. Since the positions of all cores and routers are pre-defined in our mesh-based network, we represent the position of each port with a coordinate. For a signal path $s \in S$, we denote the Euclidean distance between every two sequential ports p_i and p_j in P_s as $D(p_i, p_j)$. Then, we introduce a continuous variable pl_s to represent the propagation loss of a signal path s and calculate it as follows:

$$pl_s = L_P * \sum_{p_i, p_j \in P_s} D(p_i, p_j) \tag{6}$$

where L_P denotes the propagation loss parameter.

Second, we consider the other losses within a router. When a $s \in S$ passes a $r \in R$, the insertion loss is related to the selected router option. For example, the signal path from injection to the south has different insertion loss values in the router options shown in Figure 4(b) - (d). Therefore, for each $s \in S$, if a router $r \in R_s$ along the signal path is implemented as a $t \in R_{lib}$, we calculate the insertion loss that happens in its passed router and denote it as $L_{r,t,s}$. Then, we introduce a continuous variable rl_s to represent the insertion loss that happens in all passed routers of the signal path and model it as follows:

$$rl_s = \sum_{r \in R_s} \sum_{t \in R_{lib}} L_{r,t,s} * b_{r,t} \tag{7}$$

For each $s \in S$, we introduce a continuous variable il_s to represent its insertion loss and model it with the following constraints:

$$\forall s \in S : il_s \ge pl_s + rl_s - (1 - b_s) * \Xi \tag{8}$$

where Ξ is a very large auxiliary number. Only when a signal path is selected, i.e., $b_s = 1$ the insertion loss of the signal path is considered valid.

To model the worst-case insertion loss value among all signal paths, we introduce a continuous variable *maxil* and model it with the following constraints:

$$\forall\ c_i,\ c_j \in C,\ \forall\ s \in S_{c_i, c_j}:\ \ maxil \ge il_s \tag{9}$$

• *Optimization Function*

Our optimization objectives are the worst-case insertion loss and the MRR usage. We formulate our optimization function as follows:

$$Min : \alpha * maxil + \beta * i_{mrr} \tag{10}$$

where α and β are two weight coefficients to change the optimization preference.

3.2 Wavelength Assignment

Based on the selected signal path options and router options, we propose an ILP model to configure the radius of each MRR and assign the wavelengths to the signal paths. We introduce the variables and constraints of our ILP model as follows:

At the beginning, we introduce a set $\mathbb{S}$ for all selected signal paths and a set Λ for wavelengths. For each $s \in \mathbb{S}$ and $\lambda \in \Lambda$, we introduce a binary variable $b_{s,\lambda}$ to indicate if the signal path uses the wavelength λ. Considering that each signal path should be assigned exactly a wavelength, we introduce the following constraints:

$$\forall s \in \mathbb{S}:\ \ \sum_{\lambda \in \Lambda} b_{s,\lambda} = 1 \tag{11}$$

Similarly, we introduce a set $\mathbb{M}$ for all MRRs in the chosen router options and a set $\mathbb{R}$ for radii. For each $m \in \mathbb{M}$, we introduce a binary variable $b_{m,r}$ that indicates if an MRR m is assigned with a radius r. Then we model that each MRR is assigned exactly a radius with the following constraints:

$$\forall m \in \mathbb{M}: \quad \sum_{r \in \mathbb{R}} b_{m,r} = 1 \tag{12}$$

If some signal paths overlap at any waveguide section, they should use different wavelengths to avoid data collision. For each $s \in \mathbb{S}$, we find the signal paths that overlap with s and store them in a set $\mathbb{S}_s^{overlap}$. We introduce the following constraints to prevent the overlapping signal paths from using the same wavelengths:

$$\forall s \in \mathbb{S},\ \lambda \in \Lambda: \quad b_{s,\lambda} + \sum_{s' \in \mathbb{S}_s^{overlap}} b_{s',\lambda} \le 1 \tag{13}$$

For each $s \in \mathbb{S}$, we create a set $\mathbb{M}_s^{on}$ for its on-resonance MRRs and a set $\mathbb{M}_s^{off}$ for its off-resonance MRRs. For each $\lambda \in \Lambda$, we find the MRR radii that resonate to the wavelength and store them in a set $\mathbb{R}_\lambda^{on}$. If a signal path uses a wavelength, all on-resonance MRRs of the signal path must use the radii that resonate to the wavelength, and all off-resonance MRRs should avoid using those radii. Then, we model that with the following constraints:

$$\forall s \in \mathbb{S}: \quad \sum_{m \in \mathbb{M}_s^{on}} \sum_{r \in \mathbb{R}_\lambda^{on}} b_{m,r} \ge |\mathbb{M}_s^{on}| - (1 - b_{s,\lambda}) * \Xi \tag{14a}$$

$$\sum_{m \in \mathbb{M}_s^{on}} \sum_{r \in \mathbb{R}_\lambda^{on}} b_{m,r} \le |\mathbb{M}_s^{on}| + (1 - b_{s,\lambda}) * \Xi \tag{14b}$$

$$\sum_{m' \in \mathbb{M}_s^{off}} \sum_{r \in \mathbb{R}_\lambda^{on}} b_{m',r} \ge 0 - (1 - b_{s,\lambda}) * \Xi \tag{14c}$$

$$\sum_{m' \in \mathbb{M}_s^{off}} \sum_{r \in \mathbb{R}_\lambda^{on}} b_{m',r} \le 0 + (1 - b_{s,\lambda}) * \Xi \tag{14d}$$

where Ξ is a very large auxiliary number. If a signal path $s \in \mathbb{S}$ is assigned with a wavelength $\lambda \in \Lambda$, i.e. $b_{s,\lambda} = 1$, all on-resonance MRRs of the signal path should be configured with any of the radii in $\mathbb{R}_\lambda^{on}$, i.e., the left-hand sides of Eq. 14a and 14b are forced to $|\mathbb{M}_s^{on}|$, and no off-resonance MRRs of s can use the radii in $\mathbb{R}_\lambda^{on}$, i.e. the left-hand sides of Eq. 14c and 14d are forced to 0.

For each $\lambda \in \Lambda$, we introduce a binary variable b_λ to indicate if any signal paths use a wavelength and model it as follows:

$$\lambda \in \Lambda: \quad |\mathbb{S}| * b_\lambda \ge \sum_{s \in \mathbb{S}} b_{s,\lambda} \tag{15}$$

where $|\mathbb{S}|$ denotes the total number of all selected signal paths. If at least a signal path s is assigned with λ, i.e. $\sum_{s \in \mathbb{S}} b_{s,\lambda} \ge 1$, the corresponding constraint will force b_λ to be 1.

To minimize the wavelength usage, we formulate our optimization function as follows:

$$Min: \sum_{\lambda \in \Lambda} b_\lambda \tag{16}$$

4 EXPERIMENTAL RESULTS

We implemented our method in C++ and solved our MILP and ILP models with an optimization solver, Gurobi [21]. The coefficients in Eq. 10 are set to 1 and 0.1, respectively[2]. In Section 4.1, we compare our method to two state-of-the-art co-design methods: PSION+ [8] and CoDesign[7], for a 16-core network, which is a benchmark commonly used in the related works. For a fair comparison, we apply the same power model, communication requirements, physical constraints, and loss parameters in PSION+ [8]. In Section 4.2, we illustrate the efficiency of using multi-resonance MRRs by comparing our method to a baseline, which does not employ multi-resonance MRRs for three networks. All experiments in this paper were carried out in a 3.6 GHz CPU.

[2]Considering that i_{mrr} is greater than $maxil$, it is assigned with a smaller number to balance the optimization preference in our MILP model.

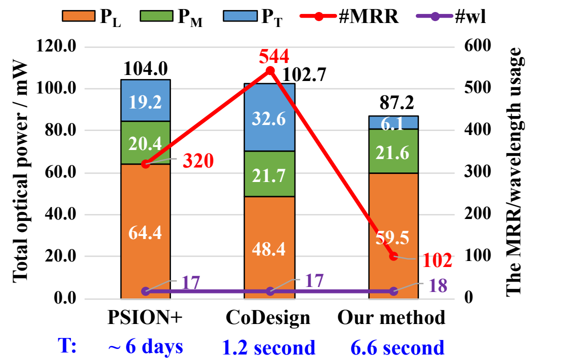

Figure 5: Total optical power and MRR usage in PSION+, CoDesign, and our method for the 16-core network with 240 communications.

4.1 Comparison to State-of-the-art Methods

We compare our method to PSION+ and CoDesign in terms of optical power consumption, MRR usage, wavelength usage, and synthesis time. Figure 5 shows the comparison results, where P_L denotes the total laser power, including the power distribution networks, P_T denotes the static MRR thermal tuning power, P_M denotes the static power of modulators and demodulators, #MRR denotes the number of MRRs, #wl denotes the number of wavelengths, and T denotes the program runtime. All power values are denoted in mW.

As shown in Figure 5, our method outperforms two state-of-the-art design methods in improving energy efficiency. Compared to PSION+, our method decreases 14% the total optical power due to the reduction in laser power and MRR tuning power. As introduced before, the laser power is defined by the worst-case insertion loss, and MRR tuning power is determined by the MRR usage. Thanks to our MILP model that optimizes the worst-case insertion loss, our method decreases the laser power versus PSION+ by 8%. For the MRR tuning power, our method significantly reduces the MRR usage compared to PSION+, which is mainly driven by using multi-resonance MRRs, where a single MRR can route signals on multiple wavelengths. Moreover, PSION+ suffers large computational complexity and requires six days to synthesize the 16-core network, while our method can finish the design within several seconds since we adopt the mesh structure and existing optical routers.

Compared to CoDesign, our method reduces the total optical power by about 13%, which is driven by reducing MRR usage. Our method decreases MRR usage by 79% versus CoDesign, which significantly reduces MRR tuning power. Compared to both state-of-the-art design methods, our method has a comparative wavelength usage thanks to our ILP model, which minimizes the number of wavelengths.

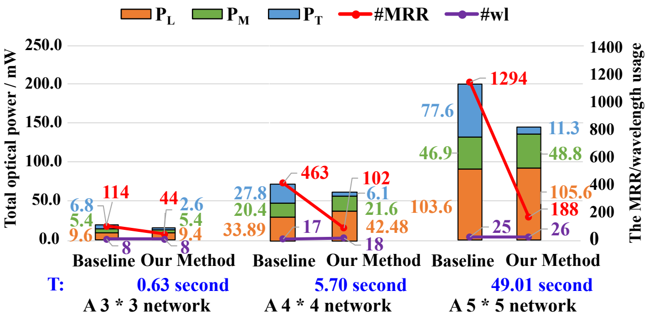

Figure 6: Comparison results between a baseline and our method for three mesh-based networks.

4.2 Comparison to a Baseline

To evaluate the efficiency of using multi-resonance MRRs, we compare our method to a baseline, which does not use any multi-resonance MRRs. For a fair comparison, the signal paths and routers in the baseline are exactly the same as those in our method. In the baseline, if multiple signals need to be on-resonance to MRRs at a place, we apply the way proposed in [20] to add as many MRRs as the number of signals at the place. Then, we assign the wavelengths to the signals using our ILP model. We tested them for three mesh-based network sizes: 9, 16, and 25 cores. For each network, we consider the full connectivity, i.e., a core sends signals to all other cores, apply the power model proposed in [8], and use the loss parameters in [20].

Figure 6 shows the comparison results between the baseline and our method. Generally, our method, which uses multi-resonance MRRs, reduces the MRR usage significantly compared to the baseline. For example, in the 5×5 network, our method with an 85% reduction in MRR usage decreases the total optical power consumption by 27% compared to the baseline. On the contrary, the number of MRRs in the baseline drastically increases as the size of networks rises, which causes a significant increase in optical consumption. That indicates the benefits of using multi-resonance MRRs. Last but not least, our method and the baseline have almost the same wavelength usage, which is optimized by our ILP model.

5 CONCLUSION

In this work, we propose an efficient design method, which synthesizes mesh-based WRONoC networks. Taking advantage of the mesh structure and existing ONoC routers, our method can greatly reduce computational complexity and focus on routing the signal paths with minimized insertion loss and MRR usage. Moreover, we make use of multi-resonance MRRs for the signals that require to be coupled at the same places to avoid high MRR usage. The experimental results show that our method outperforms two state-of-the-art design methods in both energy and computational efficiency. For a 16-core network, our method decreases the total optical power compared to the state-of-the-art methods by reducing the MRR usage. Furthermore, our method can synthesize a 16-core network in a few seconds, while a state-of-the-art method requires six days.

ACKNOWLEDGEMENTS

This work is supported by the Deutsche Forschungsgemeinschaft (DFG, German Research Foundation) – Project Number 496766278.

REFERENCES

[1] Sebastian Werner, Javier Navaridas, and Mikel Luján. A Survey on Optical Network-on-Chip Architectures. *ACM Computing Surveys*, 50(6), December 2017.
[2] Near Margalit, Chao Xiang, Steven M. Bowers, Alexis Bjorlin, Robert Blum, and John E. Bowers. Perspective on the future of silicon photonics and electronics. *Applied Physics Letters*, 118(22):220501, 06 2021.
[3] Tsun-Ming Tseng, Alexandre Truppel, Mengchu Li, Mahdi Nikdast, and Ulf Schlichtmann. Wavelength-routed optical nocs: Design and eda — state of the art and future directions: Invited paper. In *2019 IEEE/ACM International Conference on Computer-Aided Design (ICCAD)*, pages 1–6, 2019.
[4] Zhidan Zheng, Mengchu Li, Tsun-Ming Tseng, and Ulf Schlichtmann. ToPro: A Topology Projector and Waveguide Router for Wavelength-Routed Optical Networks-on-Chip. In *2021 IEEE/ACM International Conference On Computer Aided Design (ICCAD)*, pages 1–9, 2021.
[5] Mengchu Li, Tsun-Ming Tseng, Davide Bertozzi, Mahdi Tala, and Ulf Schlichtmann. CustomTopo: A Topology Generation Method for Application-Specific Wavelength-Routed Optical NoCs. In *2018 IEEE/ACM International Conference on Computer-Aided Design (ICCAD)*, page 1–8, New York, NY, USA, 2018.
[6] Zhidan Zheng, Mengchu Li, Tsun-Ming Tseng, and Ulf Schlichtmann. Light: A Scalable and Efficient Wavelength-Routed Optical Networks-On-Chip Topology. In *2021 Asia and South Pacific Design Automation Conference (ASP-DAC)*, page 568–573, 2021.
[7] Yu-Sheng Lu, Yan-Lin Chen, Sheng-Jung Yu, and Yao-Wen Chang. Topological structure and physical layout co-design for wavelength-routed optical networks-on-chip. *IEEE Transactions on Computer-Aided Design of Integrated Circuits and Systems*, 41(7):2237–2249, 2022.
[8] Alexandre Truppel, Tsun-Ming Tseng, Davide Bertozzi, José Carlos Alves, and Ulf Schlichtmann. Psion+: Combining logical topology and physical layout optimization for wavelength-routed onocs. *IEEE Transactions on Computer-Aided Design of Integrated Circuits and Systems*, 39(12):5197–5210, 2020.
[9] Alexandre Truppel, Tsun-Ming Tseng, Davide Bertozzi, José Carlos Alves, and Ulf Schlichtmann. PSION: Combining Logical Topology and Physical Layout Optimization for Wavelength-Routed ONoCs. In *2019 International Symposium on Physical Design (ISPD)*, page 49–56, 2019.
[10] Alexandre Truppel, Tsun-Ming Tseng, and Ulf Schlichtmann. PSION 2: Optimizing Physical Layout of Wavelength-Routed ONoCs for Laser Power Reduction. In *Proceedings of the 39th International Conference on Computer-Aided Design (ICCAD)*. Association for Computing Machinery, 2020.
[11] Mengchu Li, Tsun-Ming Tseng, Mahdi Tala, and Ulf Schlichtmann. Maximizing the Communication Parallelism for Wavelength-Routed Optical Networks-On-Chips. In *2020 Asia and South Pacific Design Automation Conference (ASP-DAC)*, pages 109–114, 2020.
[12] Bahareh Asadi, Midia Reshadi, and Ahmad Khademzadeh. A routing algorithm for reducing optical loss in photonic networks-on-chip. *Photonic Network Communications*, 34(1):52–62, Aug 2017.
[13] Huaxi Gu and Jiang Xu. ODOR: a microresonator-based high-performance low-cost router for optical networks-on-Chip. pages 203–208, 10 2008.
[14] Yiyuan Xie, Mahdi Nikdast, Jiang Xu, Wei Zhang, Qi Li, Xiaowen Wu, Yaoyao Ye, Xuan Wang, and Weichen Liu. Crosstalk Noise and Bit Error Rate Analysis for Optical Network-on-Chip. In *Proceedings of the 47th Design Automation Conference (DAC)*, DAC '10, page 657–660. Association for Computing Machinery, 2010.
[15] Huaxi Gu, Jiang Xu, and Zheng Wang. A Novel Optical Mesh Network-on-Chip for Gigascale Systems-on-Chip. In *APCCAS 2008 - 2008 IEEE Asia Pacific Conference on Circuits and Systems*, pages 1728–1731, 2008.
[16] Huaxi Gu, Mo Morton, Jiang Xu, and Wei Zhang. A Low-power Low-cost Optical Router for Optical Networks-on-Chip in Multiprocessor Systems-on-Chip. pages 19–24, 01 2009.
[17] Xianfang Tan, Mei Yang, Lei Zhang, Yingtao Jiang, and Jianyi Yang. On a Scalable, Non-Blocking Optical Router for Photonic Networks-on-Chip Designs. In *2011 Symposium on Photonics and Optoelectronics (SOPO)*, pages 1–4, 2011.
[18] W. Bogaerts, P. De Heyn, T. Van Vaerenbergh, K. De Vos, S. Kumar Selvaraja, T. Claes, P. Dumon, P. Bienstman, D. Van Thourhout, and R. Baets. Silicon microring resonators. *Laser & Photonics Reviews*, 6(1):47–73, 2012.
[19] Marta Ortín-Obón, Mahdi Tala, Luca Ramini, Víctor Viñals-Yufera, and Davide Bertozzi. Contrasting Laser Power Requirements of Wavelength-Routed Optical NoC Topologies Subject to the Floorplanning, Placement, and Routing Constraints of a 3-D-Stacked System. *IEEE Transactions on Very Large Scale Integration (VLSI) Systems*, PP:1–14, 03 2017.
[20] Mahdi Nikdast, Jiang Xu, Luan Huu Kinh Duong, Xiaowen Wu, Xuan Wang, Zhehui Wang, Zhe Wang, Peng Yang, Yaoyao Ye, and Qinfen Hao. Crosstalk Noise in WDM-Based Optical Networks-on-Chip: A Formal Study and Comparison. *IEEE Transactions on Very Large Scale Integration (VLSI) Systems*, 23(11):2552–2565, 2015.
[21] Inc. Gurobi Optimization. *Gurobi Optimizer Reference Manual*. http://www.gurobi.com, 2023.